THE JOURNAL OF PHYSICAL CHEMISTRY B

Article

Cite This: J. Phys. Chem. B 2018, 122, 4513−4520

pubs.acs.org/JPCB

# Chromophore-Removal-Induced Conformational Change in Photoactive Yellow Protein Determined through Spectroscopic and X-ray Solution Scattering Studies

Youngmin Kim,[†,‡,§] Prabhakar Ganesan,[†,§] Junbeom Jo,[†,‡] Seong Ok Kim,[†,‡] Kamatchi Thamilselvan,[†,‡] and Hyotcherl Ihee*[,†,‡]

[†]Department of Chemistry and KI for the BioCentury, Korea Advanced Institute of Science and Technology (KAIST), Daejeon 34141, Republic of Korea

[‡]Center for Nanomaterials and Chemical Reactions, Institute for Basic Science (IBS), Daejeon 34141, Republic of Korea

Supporting Information

**ABSTRACT:** Photoactive yellow protein (PYP) induces negative phototaxis in *Halorhodospira halophila* via photoactivation triggered by light-mediated chromophore isomerization. Chromophore isomerization proceeds via a volume-conserving isomerization mechanism due to the hydrogen-bond network and steric constraints inside the protein, and causes significant conformational changes accompanied by N-terminal protrusion. However, it is unclear how the structural change of the chromophore affects the remote N-terminal domain. To understand photocycle-related structural changes, we investigated the structural aspect of chromophore removal in PYP because it possesses a disrupted hydrogen-bond network similar to that in photocycle intermediates. A comparison of the structural aspects with those observed in the photocycle would give a clue related to the structural change mechanism in the photocycle. Chromophore removal effects were assessed via UV−vis spectroscopy, circular dichroism, and X-ray solution scattering. Molecular shape reconstruction and an experiment-restrained rigid-body molecular dynamics simulation based on the scattering data were performed to determine protein shape, size, and conformational changes upon PYP bleaching. Data show that chromophore removal disrupted the holo-PYP structure, resulting in a small N-terminal protrusion, but the extent of conformational changes was markedly less than those in the photocycle. This indicates that disruption of the hydrogen-bond network alone in bleached PYP does not induce the large conformational change observed in the photocycle, which thus must result from the organized structural transition around the chromophore triggered by chromophore photoisomerization along with disruption of the hydrogen-bond network between the chromophore and the PYP core.

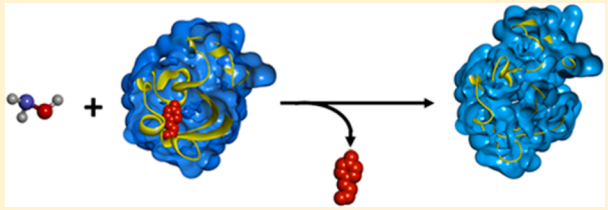

## INTRODUCTION

Photoactive yellow protein (PYP) is a member of the xanthopsin photoreceptor family and mediates negative phototaxis in *Halorhodospira halophila* in response to blue light.[1] It is a useful photoresponsive module for optogenetic tools owing to its small size (14 kDa; 125 amino acid residues), high solubility, and capacity for extensive structural change.[2−4] Hence, PYP and its photocycle have been extensively investigated with various spectroscopic and crystallographic techniques.[5−14] Photomediated structural changes in PYP are initiated with the excitation of the chromophore, p-coumaric acid (4-hydroxycinnamic acid), followed by chromophore trans−cis isomerization.[2,6] Spectroscopic and crystallographic data suggest that the chromophore exists as a deprotonated phenolate anion in the dark state,[15] and displays a yellow color by adopting a trans conformation.[16] The chromophore interacts with adjacent residues through hydrogen bonds (Tyr42, Glu46, and Cys69) and hydrophobic interactions (Tyr98, Thr50, Arg52, Phe62, Val66, Ala67, Cys69, Phe96, and Tyr98) (Figure 1a,b and Supporting Information Table S1). These interactions may enhance the compactness and stability of holo-PYP as compared to apo-PYP (PYP without the chromophore). Since the chromophore is embedded in a cavity inside the protein with such interactions, the conformational mobility of the chromophore is severely restricted by interactions with the surrounding amino acids, including hydrogen-bond interactions and steric constraints. Consequently, the isomerization pathway proceeds via volume-conserving isomerization pathways instead of a simple one-bond flip to minimize the volume swept out by the chromophore.[11] The mechanical force caused by volume-conserving isomerization seems to be transferred to the N-terminus, which is distal from the chromophore and ultimately causes N-terminal protrusion. However, it is still unclear how the structural changes in the chromophore affect the remote N-terminal structure of the protein.

**Received:** February 21, 2018
**Revised:** April 4, 2018
**Published:** April 12, 2018





DOI: 10.1021/acs.jpcb.8b01768
J. Phys. Chem. B 2018, 122, 4513−4520

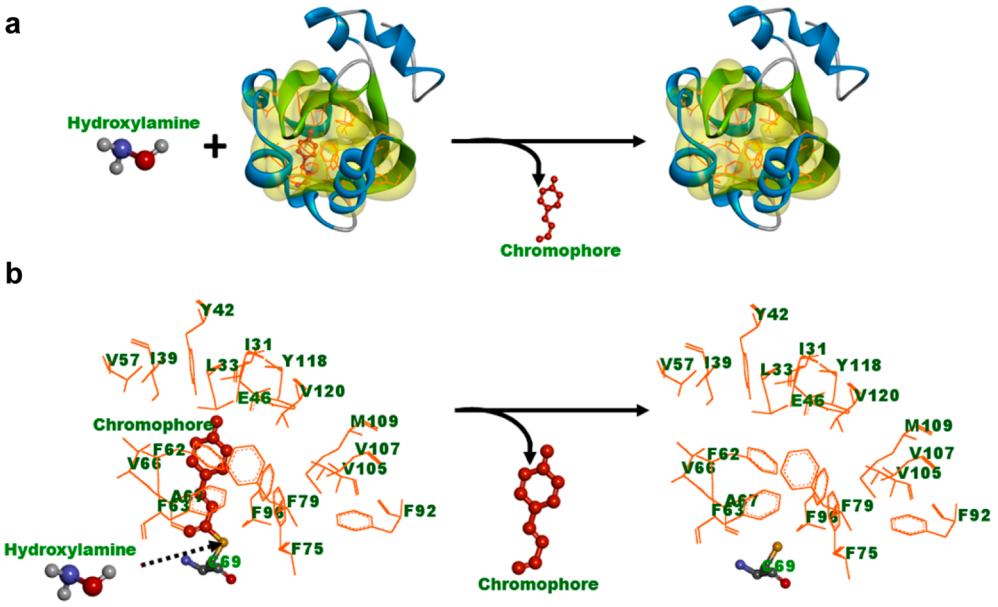


**Figure 1.** Schematic representation of chromophore removal from PYP. (a) Schematic representation of the chromophore removal in PYP by hydroxylamine and (b) close-up view of the chromophore region. Residues that interact with the chromophore via hydrogen bonding and hydrophobic interactions are labeled.

Previous studies on the PYP photocycle suggested that disturbances in hydrogen-bond interactions between the chromophore and PYP core (Tyr42, Glu46, and Cys69) by light absorption significantly influence the N-terminus.[11,17−19] The chemical detachment of the chromophore is predicted to have a similar effect because the bleached PYP (chromophore-removed PYP) also possesses a disrupted hydrogen-bond network similar to that in photocycle intermediates. Hence, it is of interest to compare the structural aspects of bleached PYP with that of photocycle intermediates. Therefore, to better understand the structural change during the photocycle, we investigated the conformational changes in PYP induced by chromophore removal and compared the bleached PYP structure with that of photocycle intermediates, especially $pB_2$. The $pB_2$ intermediate, which is the purported signaling state, shows the largest conformational change accompanied by N-terminal protrusion and the longest relaxation time during the photocycle in solution. The structural aspect of chromophore-removed PYP corresponds to the effect of hydrogen-bond disruption between the chromophore and surrounding amino acids without the effect of trans−cis chromophore isomerization. Thus, this study might provide insights into the effect of mechanical force generated by trans−cis isomerization and the mechanisms underlying the conformational changes, especially protrusion of the N-terminus during the PYP photocycle.

The chromophore binds to PYP via a covalent bond that is resistant to denaturing reagents or boiling, but can be irreversibly dissociated through reaction with hydroxylamine ($NH_2$−OH), dithiothreitol, and performic acid, as well as under high pH.[3,16] Hydroxylamine specifically cleaves the thioester bond (R−CO−S−R′) between the chromophore and the protein (Figure 1a,b), resulting in a thiol group (R′−SH) and hydroxamic acid (R−CO−NH−OH).[3] Thus, the detachment of the chromophore from holo-PYP using hydroxylamine should provide an opportunity to investigate conformational changes during chromophore detachment.

In the present study, we investigated the conformational change in PYP induced by chromophore removal with hydroxylamine, using UV−vis spectroscopy, circular dichroism (CD), X-ray solution scattering, and experiment-restrained rigid-body MD simulations to determine the structural contribution of chromophore binding. Furthermore, we compared the structural aspects of bleached PYP with those of photocycle intermediates such as $pB_2$ to better understand the mechanism underlying the photocycle of PYP, especially the formation of $pB_2$ in solution. UV−vis spectroscopic data were collected after initiation of bleaching with hydroxylamine as a function of time to obtain kinetic information related to protein structure and conformational changes in solution.

## EXPERIMENTAL METHODS

**Small-Angle X-ray Scattering (SAXS).** SAXS data $\{I(q)$ vs $q$ $[=(4\pi/\lambda)\sin\theta]$, where $q$ and $2\theta$ are the scattering vector and scattering angle, respectively$\}$ were obtained at the 4C SAXS II beamline at Pohang Light Source (PLS-II) in Korea. The X-ray wavelength was 0.7336 Å (16.90 keV). A two-dimensional charge-coupled detector (Rayonix, Evanston, IL) was used, and the sample-to-detector distance was set at 1 or 4 m. The $q$ range of the obtained data was 0.03−0.6 $Å^{-1}$. Data were obtained with a PYP concentration of 10 mg/mL, using the supernatant obtained after centrifugation at over 10 000 $g$ for 10 min to remove aggregates.

The SAXS profiles of the holo and bleached PYP structure were obtained through a static X-ray solution scattering experiment by using a flow cell system (Figure S1). Briefly, the flow-cell system contained continuous injection (syringe pump and syringe) and measuring (capillary system) components prepared in the beamline. The PYP sample solution was injected into the capillary system at a precisely controlled speed (100 $\mu$L per min). The capillary was 1.0 mm thick, and the exposure time was 10 or 60 s. The solution buffer contained 20 mM Tris pH 7.0 and 20 mM NaCl.

**SAXS Analysis and Molecular Shape Reconstruction.** The SAXS data were processed and analyzed using the ATSAS


DOI: 10.1021/acs.jpcb.8b01768
J. Phys. Chem. B 2018, 122, 4513−4520

package (http://www.embl-hamburg.de/biosaxs/software.html).[20−23] One-dimensional scattering data $I(q)$ as a function of $q$ were obtained by radial averaging. Scattering intensities from the buffer solution were measured for background. The $I(q)$ sample data were extrapolated to the point where $q = 0$ by GNOM. The Rg and particle distance distribution function $P(r)$ were then calculated through indirect Fourier transformation. The $q$ and real space ranges for holo-PYP were 0.0319−0.3093 Å$^{-1}$ and 0.00−39.00 Å, respectively, and those for bleached PYP were 0.0332−0.2899 Å$^{-1}$ and 0.00−46.54 Å, respectively. The maximum dimension ($D_{max}$), the distance $r$ where $P(r) = 0$ for the particle, was determined from the $P(r)$ function on the basis of a previously determined PYP crystal structure. Because indirect transformation was used to calculate the RDFs (radial distribution function), excessively large $D_{max}$ values were discarded. Simulated annealing was performed with a $q$ range of 0.031−0.309 Å$^{-1}$ (holo-PYP) and 0.033−0.289 Å$^{-1}$ (bleached PYP) using optimal RDFs in the DAMMIF package[24] to generate molecular envelope models. Representative structures were constructed by superimposing the raw DAMMIF results onto a template structure using DAMSEL and DAMSUP.

There were 20 independently calculated low-resolution dummy atomic models averaged with DAMAVER.[25] A representative structure with high-probability densities was then filtered using DAMFILT. The reconstructed molecular envelopes were compared with models obtained from experiment-restrained rigid-body MD simulations to visualize the conformational change caused by bleaching at the atomic level. The molecular envelopes, crystal structures, and experiment-restrained rigid-body MD simulation results were superimposed using SUPCOMB.[26]

**SAXS Difference Curve Analysis with an Experiment-Restrained Rigid-Body MD Simulation.** High-resolution structural changes between the holo and bleached PYP were obtained from experiment-restrained rigid-body MD simulations (see Supporting Information). The theoretical X-ray scattering curve calculated on the basis of the PYP crystal structure (PDB code: 2PHY) is identical to the experimental X-ray scattering curve of holo-PYP, within the error range. Therefore, we used the crystal structure as holo-PYP structure in experiment-restrained rigid-body MD simulations. We manually removed the chromophore from the holo structure and used the resulting structure as the initial structure to refine the bleached PYP structure. In our approach, two or three amino acids in the loop region and 3−10 amino acids in the $\alpha$ helix and $\beta$ sheet were grouped into one rigid body in the initial PYP structure to reduce the MD simulation time and parameters. In total, ∼30 rigid bodies were used in the experiment-restrained rigid-body MD simulations. The CRYSOL program[27] was used to generate the X-ray scattering curve during the experiment-restrained rigid-body MD simulations. The calculated difference scattering curve was acquired by subtracting the scattering curve of the holo-PYP from that of the expected bleached PYP structure. The difference between the calculated difference scattering curve and the experimental difference scattering curve was used to evaluate the MD force term along with the usual van der Waals force term. Thereafter, we fitted the experimental data by altering the CRYSOL parameters, i.e., the radius of the atomic group, the contrast in the hydration shell, the excluded volume, and the scaling factor between the experimental and theoretical results. We used the MINUIT package in the ROOT software[28] from CERN. The experiment-restrained rigid-body MD simulation and CRYSOL parameter fit were performed iteratively until the smallest $\chi$-square value was reached. In this way, we determined the best model where the theoretical difference scattering curve agreed with the experimental SAXS difference curve.

## RESULTS

**Colorimetric and UV−Vis Spectroscopy Analysis of PYP Bleaching.** Preliminary tests following a previous work showed that bleaching of PYP with hydroxylamine in a phosphate buffer eventually resulted in protein aggregation.[3] Hence, we optimized the protocol to prevent such aggregation. Specifically, the optimized protocol required higher concentrations of the buffer salt (400 mM, Tris, pH 7.0) and hydroxylamine concentration lower than 450 mM, which led to complete bleaching of the PYP solution without any aggregation (Figure 2a and Figure S2). If hydroxylamine concentration was excessively increased beyond the optimized condition, e.g., beyond 450 mM, aggregation was observed. Peaks at 318 and 306 nm corresponding to the thioester bond in the PYP UV−vis spectrum disappeared due to hydroxylamine bleaching.[3] In addition, the effect of hydroxylamine concentration on bleaching was determined by a UV−vis spectral analysis at four different concentrations of hydroxylamine (350, 400, 450, and 500 mM) (Supporting Information Figure S3a−d). The decay constant was fitted by using the absorbance at 446 nm for each data set (Supporting Information Figure S3e,f). The results indicate that the chromophore-cutting process is a pseudo-first-order reaction. White aggregated particles observed when hydroxylamine concentration over 450 mM was used may have further impeded chromophore cleavage. We estimated that aggregation of PYP slightly increased the decay time constant if hydroxylamine concentration over 450 mM was used. In addition, our results showed only a single decay constant exists

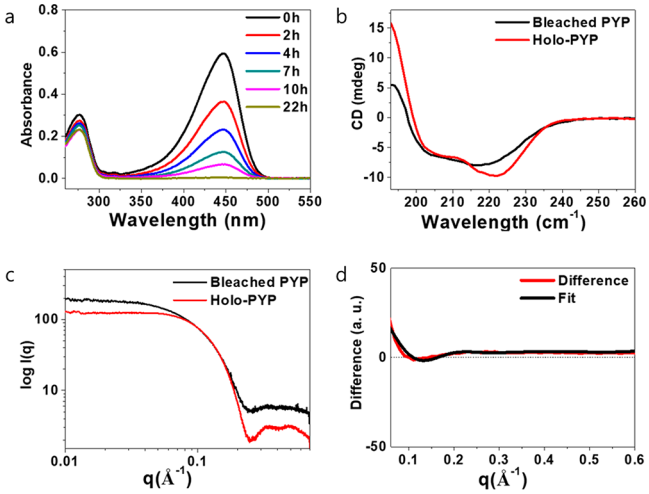


**Figure 2.** Measurement of bleached PYP and holo-PYP using UV−vis spectroscopy, CD, and SAXS. (a) PYP bleaching as determined through UV−vis spectrum over 22 h in 300 mM hydroxylamine. Spectra at selected time points (0, 2, 4, 7, 10, and 22 h) are shown. (b) Circular dichroism spectra of PYP before (red) and after (black) the bleaching reaction. (c) Static SAXS curves of holo-PYP (red) and bleached PYP (black). (d) Difference curve (red) in SAXS curves and the fit curve from experiment-restrained rigid-body MD simulation (black).



DOI: 10.1021/acs.jpcb.8b01768
J. Phys. Chem. B 2018, 122, 4513−4520

under various bleaching conditions, indicating that the reaction proceeds in a two-state process without involvement of any intermediates detectable with the available time resolution.

**Structural Analysis by Matrix-Assisted Laser Desorption/Ionization (MALDI) and CD.** The molecular weight of PYP without the chromophore is 13.88 kDa, as determined from the PYP amino acid sequence without the chromophore, using the Protein Molecular Weight Calculator (sciencegateway.org). The MALDI data showed that the molecular weight of bleached PYP was measured as 13.90 kDa and that of holo-PYP as 14.0 kDa (Supporting Information Figure S4), confirming that the chromophore, whose weight is about 0.1 kDa, is released from PYP after the bleaching reaction without any peptide bond cleavages.

We examined the changes in the protein secondary structure, using CD (Figure 2b). Notably, bleached PYP displayed a somewhat stable secondary structure, but showed a slight reduction in helical structure (deduced from the peak decrease near ~223 nm) and an increase in random coils and $\beta$ sheets (deduced from the peak increase near ~195 nm). The structure did not entirely unfold because of bleaching, although it appeared to undergo partial unfolding. This observation confirmed that chromophore removal from PYP induces perturbations in the protein structure, possibly owing to the cleavage of hydrogen bonds and hydrophobic interactions between the chromophore and the protein, thereby destabilizing the intact structure of the PYP.

**Static Small-Angle X-ray Scattering (SAXS).** SAXS was performed to investigate the structural changes in holo-PYP, which occur in response to hydroxylamine treatment (Figure 2c). We confirmed that holo and bleached PYP had Rg (radius of gyration) values of 14.6 and 14.7, respectively, as determined using the PRIMUS program in the ATSAS software package. To detect the scattering change, the difference in the scattering profile was obtained by subtracting the scattering of the holo-PYP sample from that of the bleached sample. Prior to subtraction, the data were normalized at $q$ = 0.095 Å$^{-1}$ because time-resolved SAXS data intersect at the $q$ = 0.095 Å$^{-1}$ (Figure 2d and Supporting Information Figure S5). Moreover, the difference curves derived using normalization at other $q$ points could not be satisfactorily fit by experiment-restrained rigid-body MD simulations. Notably, the scattering intensity decreased in the region from $q$ = ~ 0.04 to 0.12 Å$^{-1}$ and slightly increased thereafter. Furthermore, we conducted both low-resolution shape reconstruction and an experiment-restrained rigid-body MD simulation to investigate the structure and to accurately estimate the structural changes.

**Low-Resolution Shape Reconstruction of Holo-PYP and Bleached PYP.** The SAXS shape determination method was used to reconstruct low-resolution molecular envelopes of both holo-PYP and bleached PYP. GNOM in ATSAS was used to determine the initial input data for DAMMIF, which was implemented to extract the optimized structures (Figure 3a–c and Figure S6a–d).

Slight protrusions were observed in the low-resolution model of bleached PYP, compared to that of holo-PYP, which explains the slightly increased Rg value for bleached PYP. However, the low-resolution model cannot show which specific part of PYP protrudes. To accurately determine such detailed structural information, we used an experiment-restrained rigid-body MD simulation.

**Experiment-Restrained Rigid-Body MD Simulation of SAXS Data.** Conformational changes of the bleached PYP were determined using experiment-restrained rigid-body MD simulations. The results are shown in Figures 2d and 3e. A comparison of the holo-PYP structure with the fit structure of bleached PYP shows that they are different in that bleached PYP has a small protrusion in the N-terminus (Figure 3f). This result indicates that the disruption of the thioester bond between cysteine and the chromophore and the subsequent loss of hydrogen bonds and hydrophobic interactions between the chromophore and PYP result in the conformational change in the bleached PYP.

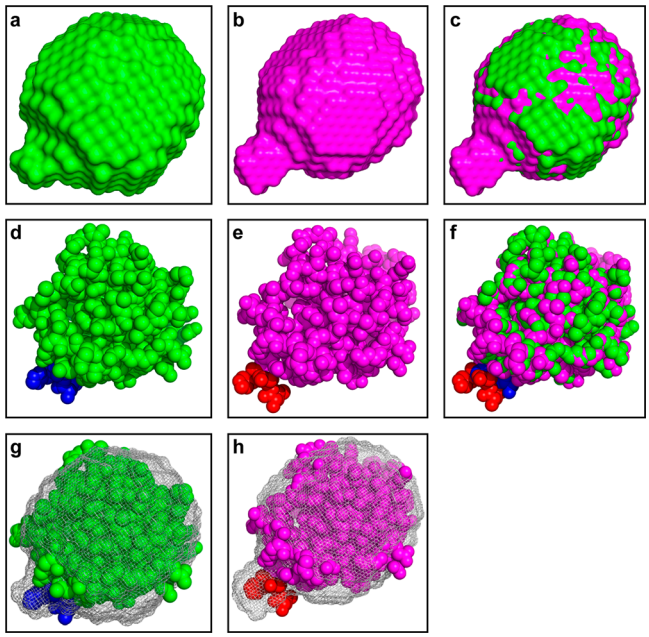


**Figure 3.** Molecular structure modeling from a low-resolution shape reconstruction and an experiment-restrained rigid-body MD simulation. (a–c) Filtered, low-resolution reconstructed shapes of holo-PYP (a), bleached PYP (b), and the superimposed image (c) from DAMMIF. (d–f) Structural representation of holo-PYP (2PHY) (d), bleached PYP from experiment-restrained rigid-body MD simulation (e), and its superimposed image (f). (g, h) Comparison of shapes from low-resolution shape reconstruction (mesh) and experiment-restrained rigid-body MD simulation (sphere-dot) with regard to holo-PYP (g) and bleached PYP (h). Blue and red colors indicate three amino acids at the N-terminal region of holo-PYP and bleached PYP, respectively.

## DISCUSSION

The essential step in photoreception by proteins is the storage of energy from photons. PYP differs from other photoreceptor proteins in that its chromophore undergoes photoisomerization when excited, and the absorbed photons cause a reversible structural rearrangement in the absence of other substrates or redox activity.[3] Thus, investigating the changes in protein structure and contribution to the reaction mechanism in the absence of the chromophore is of interest.

Previous studies reported that the yellow color of PYP solution results from molecular events associated with the conjugation, insertion of the chromophore in the hydrophobic core, and deprotonation.[15] To generate the holo-protein from the apoprotein, chromophore binding to a protein's hydrophobic core region and the formation of a thioester bond between the chromophore and Cys69 in PYP are required.[3] Hydroxylamine cleaves the thioester bond between Cys69 and the chromophore. Furthermore, hydroxylamine cleavage is


DOI: 10.1021/acs.jpcb.8b01768
J. Phys. Chem. B 2018, 122, 4513–4520

accompanied by the elimination of hydrogen bonds between the chromophore and Glu46, Tyr42, and Cys69, and discoloration of the PYP solution (decreasing the absorbance at 446 nm). A previous UV−vis spectroscopy study reported that hydroxylamine-mediated holo-PYP bleaching decreases the absorbance at 446 nm[3], but kinetics and conformational changes of PYP associated with the bleaching process are yet unknown. The time-resolved UV−vis analysis revealed that the bleaching occurred with one decay constant, indicating that the conformational change associated with the bleaching phenomenon occurs in a two-state process with a pseudo-first-order reaction depending on the ratio between hydroxylamine and PYP concentrations (Supporting Information Figure S2a−f). In addition, MD simulation data obtained through GROMACS to mimic the bleaching phenomenon by cleaving the bond between the chromophore and PYP core indicate that the chromophore migrated to the solvent through a pore surrounded by Lys60, Gln5, Arg52, Gln99, and Cys69 without any significant retention (Supporting Information Figure S7a,b and Table S2).

The bleaching-induced conformational change in PYP is evident from the CD and X-ray solution scattering data. CD results indicate chromophore removal from PYP induces perturbations in protein structure. SAXS shape reconstruction confirmed the presence of a small protrusion in bleached PYP (Figure 3a−c). The Rg calculated from the SAXS data appeared to slightly increase after the bleaching reaction; however, it did not indicate any large-scale protein conformational change. The resulting protein models from the experiment-restrained rigid-body MD simulation confirm the small N-terminal protrusion (Figure 3d−f). Although the structural analyses were performed using different methods and $q$ ranges, both low-resolution shape reconstruction and the experiment-restrained rigid-body MD simulation indicated similar conformational differences between bleached and unbleached PYP (Figure 3g−h). The conformational change involving the small N-terminal protrusion occurred naturally in bleached PYP because of chromophore removal, whereas the unbleached PYP became compact owing to hydrogen bonds and hydrophobic interactions between the chromophore and the protein core. The protrusion of the N-terminal region is possibly owing to cleavage of the intramolecular interactions through chromophore removal. Cleavage of the intramolecular interaction between the chromophore and the amino acids near the chromophore by chromophore removal and the formation of a cavity in PYP by chromophore migration cause the decrease of stability of the structure in PYP. The decrease of stability may induce a partial structural change and loosen the interaction between the N-terminal region and the PYP core, resulting in a small N-terminal protrusion (Figure 4a). These results confirm that the interaction of the chromophore with amino acids in the chromophore-binding cleft via hydrogen bonds and hydrophobic interactions is important for maintaining the holo-PYP structure. The relationship between a bleaching-induced conformational change and photocycle events in PYP, particularly those related to the $pB_2$ structure, is of special interest. Comparing the bleached PYP structure with that of photocycle intermediates such as $pB_2$ might provide insights into the mechanisms underlying the conformational change, especially protrusion of the N-terminus during PYP photocycle. The photocycle is known to significantly affect the N-terminal region of the PYP via disruption of the hydrogen-bond network (chromophore, Tyr42, Glu46, and Cys69).[18,19,29] A previous

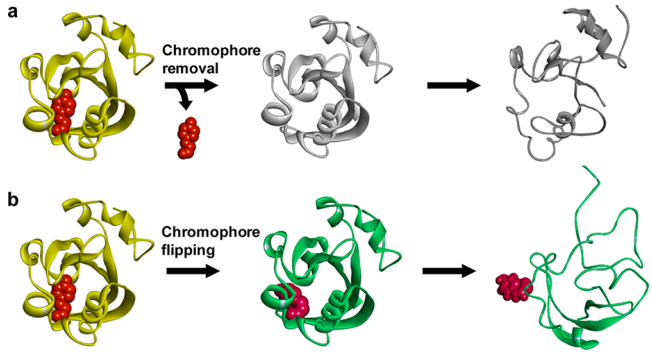


**Figure 4.** Scheme of the structural change of PYP (a) by chromophore removal and (b) by chromophore flipping upon blue-light irradiation. The chromophore is depicted as dark-red spheres. (a) The bleached PYP shows a partial structural change with a small N-terminal protrusion due to the loss of the chromophore that causes elimination of the interactions between the chromophore and the PYP core. The cleavage of the intramolecular interaction between the chromophore and amino acids near the chromophore and the formation of a cavity by chromophore migration may induce a partial structural change and loosen the interaction between the N-terminal region and the PYP core, resulting in a small N-terminal protrusion. (b) $pB_2$ shows a global structural change with a large N-terminal protrusion due to chromophore flipping. The force of the chromophore flip in holo-PYP may result in the larger global conformational change compared with the change in bleached PYP. The chromophore flipping that causes rearrangement of amino acids including Ile49, Thr50, Arg124, and Lys123 and the disruption of the hydrogen-bond network results in a larger conformational change.

study proposed that the disruption further propagates toward the N-terminal hydrogen-bond network (chromophore−Gln46−Asn43−Phe28/Leu23), thereby causing an N-terminal protrusion.[8,30,31] However, the bleached PYP structure determined in the current X-ray solution scattering study is distinct from the previously reported structure corresponding to the $pB_2$ structure,[29,32] although the former possesses a disrupted hydrogen-bond network similar to that in $pB_2$. We performed a structural superimposition to accurately identify the structural differences between the $pB_2$ structure determined from a combined measurement of NMR, DEER, and TR-WAXS in solution (PDB ID: 2KX6) and the bleached structure from experiment-restrained rigid-body MD simulation (Figure 5a). Although both structures exhibit the N-terminal protrusion because of the perturbed hydrogen-bond network, the magnitude of the protrusion is markedly larger in the $pB_2$ structure. Large conformational changes of the N-terminal region are not observed in bleached PYP. Potential energies calculated using GROMACS showed that ground-state PYP (pG) without chromophore is characterized by a lower energy than that of the $pB_2$ structure (Supporting Information Table S3). Hence, the lower free energy value in pG without chromophore is likely to prevent the transformation of bleached PYP to $pB_2$, implying that the disruption of hydrogen bonds alone in the bleached PYP is not sufficient to change the conformation to the $pB_2$ structure. Thus, the structural change in $pB_2$ is not only due to the perturbation of the hydrogen-bond network in the chromophore environment, but also it is the outcome of other molecular events such as a well-organized movement involving the chromophore in cis conformation.

Various studies have reported that the presence of the cis-chromophore generated by blue light illumination facilitates partial unfolding of the protein, whereas the trans-chromophore


DOI: 10.1021/acs.jpcb.8b01768
J. Phys. Chem. B 2018, 122, 4513−4520

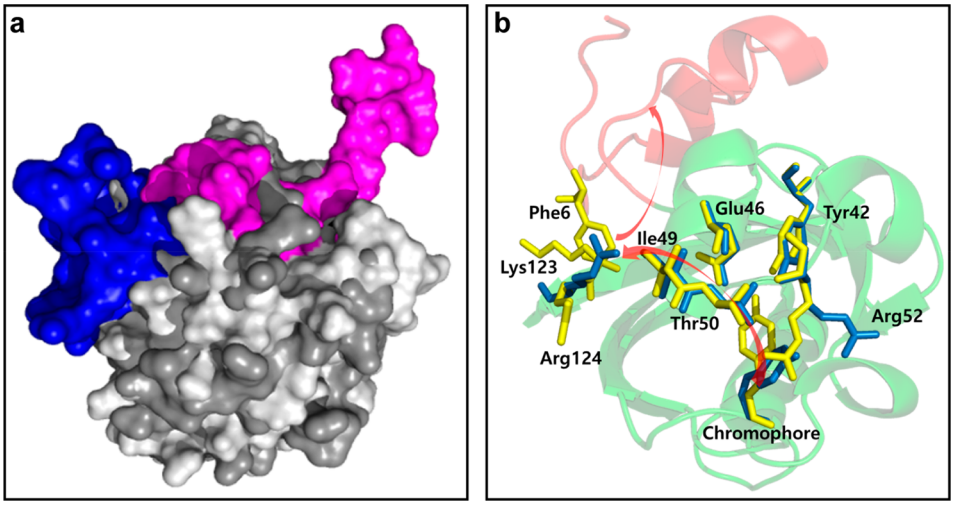


**Figure 5.** Comparison of the bleached structure and $pB_2$ structure in solution and key amino acids during photoinduced conformational changes. (a) The bleached structure from experiment-restrained rigid-body MD simulation and the $pB_2$ structure (PDB ID: 2KX6) determined using a combined measurement of NMR, DEER, and TR-WAXS is shown in the surface representation; the protein core is depicted in white (bleached structure) and gray ($pB_2$), and the N-terminal region (1−28) is depicted in blue (bleached structure) and magenta ($pB_2$), respectively. The magnitude of the N-terminal protrusion is significantly larger in the $pB_2$ structure. (b) The chromophore and key amino acids of the ground state (yellow) and the blue-shifted intermediate (blue) in the crystal structure of PYP are shown in a stick representation (PDB ID: 2PYP). The N-terminal region (1−28) is depicted in red. The chromophore hydrogen-bonded residues Tyr42 and Glu46 do not show a significant difference whereas Arg52 and Arg124 exhibited a marked difference between the blue-shifted intermediate and ground state. The rearrangement of amino acids near the chromophore can be propagated up to the N-terminal region in PYP through intramolecular interaction (red arrow; chromophore → Thr50 → Ile49 → Arg124 → Lys123 → Phe6) and can play an important role in triggering global conformational changes.

facilitates a stable, well-ordered state.[11,12] The chromophore flipping from trans to cis configuration leads to rearrangement of amino acids near the chromophore, and may disrupt the interaction between the PYP core and its N-terminal region. Hence, we examined structure displacements between a blue-shifted intermediate and the ground state in the crystal structure of PYP (PDB ID: 2PYP, solved at a resolution of 1.9 Å and a time resolution of 10 ms). The crystal structure contains both the blue-shifted intermediate (cis-chromophore) and the ground state (trans-chromophore).[33] Although large-scale global conformational changes are hindered by unit cell constraints in the crystal structure, Arg52 and Arg124, which interact with the chromophore by intramolecular interaction, exhibit a marked difference between the blue-shift intermediate and ground state (Figure 5b). This indicates that chromophore flipping causes rearrangement of amino acids in the PYP core. A previous study identified the key interaction between the N-terminal cap amino acids and $\beta$ sheet in the PYP core as a weak CH−$\pi$ interaction between the alkyl chain of Lys123 and the phenyl ring of Phe6.[34] Therefore, we suggest that the rearrangement of Arg124 by chromophore flipping through intramolecular interaction (Ile49 and Thr50) affects Lys123 conformation, thereby disrupting the weak CH−$\pi$ interaction between Lys123 of the N-terminal amino acids and Phe6 the of PYP core, which eventually results in decreased stability of the N-terminal region (Figure 5b). The decrease of stability of the N-terminal region then causes its partial unfolding. Because PYP in solution is not constrained by a crystal packing force, the decrease of stability and the unfolded structure of N-terminal region facilitates a large conformational change accompanied by an N-terminal protrusion in solution. Eventually, the chromophore flipping and amino acid rearrangements including Ile49, Thr50, Arg124, and Lys123 in concert with the disruption of the hydrogen-bond network (chromophore−Gln46−Asn43−Phe28/Leu23) are likely to cause a larger conformational change in $pB_2$ (Figure 4b).

## CONCLUSIONS

The present study shows that cleavage of the thioester bond between the chromophore and PYP core induced by hydroxylamine treatment allowed the chromophore to migrate to the solution, thereby resulting in a small N-terminal protrusion and slight change of the Rg value. These results confirm that the interaction of the chromophore with amino acids in the chromophore-binding cleft is important for maintaining the holo-PYP structure. Furthermore, the much smaller N-terminal protrusion than that of $pB_2$ suggests that the structural change of $pB_2$ cannot be explained by the disruption of the hydrogen-bond network between the chromophore and Glu46/Tyr42 alone. Our findings suggest that the organized rearrangement of amino acids that surround the chromophore by chromophore flipping, in concert with the disruption of the hydrogen-bond network, plays a critical role in the formation of the $pB_2$ structure. These findings underscore the important effect of the organized mechanical forces resulting from chromophore flipping on overall protein conformational changes.

## ASSOCIATED CONTENT

### Supporting Information

The Supporting Information is available free of charge on the ACS Publications website at DOI: 10.1021/acs.jpcb.8b01768.

Sample preparation, UV−vis spectroscopic measurements, SAXS measurements and analysis, and MD simulation for bleached PYP (PDF)

## AUTHOR INFORMATION

### Corresponding Author

*E-mail: hyotcherl.ihee@kaist.ac.kr. Phone: +82-42-350-2844.



DOI: 10.1021/acs.jpcb.8b01768
J. Phys. Chem. B 2018, 122, 4513−4520

## ORCID

Youngmin Kim: 0000-0001-8538-8435
Junbeom Jo: 0000-0002-2037-7302
Hyotcherl Ihee: 0000-0003-0397-5965


## Author Contributions

[§]Y.K. and P.G. contributed equally.

## Notes

The authors declare no competing financial interest.

## ■ ACKNOWLEDGMENTS

This study was supported by IBS-R004. We would like to thank Kyeong Sik Jin, the 4C SAXS beamline manager at PLS, for a critical discussion of our SAXS results. We thank Sang Jin Lee, So Ri Yun, and Yonggwan Kim for their help in experiments.

## ■ REFERENCES


(1) Kort, R.; Hoff, W. D.; VanWest, M.; Kroon, A. R.; Hoffer, S. M.; Vlieg, K. H.; Crielaard, W.; VanBeeumen, J. J.; Hellingwerf, K. J. The xanthopsins: a new family of eubacterial blue-light photoreceptors. *EMBO J.* **1996**, *15*, 3209−3218.

(2) Hoff, W. D.; Van Stokkum, I. H. M.; Gural, J.; Hellingwerf, K. J. Comparison of acid denaturation and light activation in the eubacterial blue-light receptor photoactive yellow protein. *Biochim. Biophys. Acta, Bioenerg.* **1997**, *1322*, 151−162.

(3) Imamoto, Y.; Ito, T.; Kataoka, M.; Tokunaga, F. Reconstitution Photoactive Yellow Protein from Apoprotein and P-Coumaric Acid-Derivatives. *FEBS Lett.* **1995**, *374* (2), 157−160.

(4) Imamoto, Y.; Kamikubo, H.; Harigai, M.; Shimizu, N.; Kataoka, M. Light-induced global conformational change of photoactive yellow protein in solution. *Biochemistry* **2002**, *41*, 13595−13601.

(5) Cordfunke, R.; Kort, R.; Pierik, A.; Gobets, B.; Koomen, G. J.; Verhoeven, J. W.; Hellingwerf, K. J. Trans/cis (Z/E) photoisomerization of the chromophore of photoactive yellow protein is not a prerequisite for the initiation of the photocycle of this photoreceptor protein. *Proc. Natl. Acad. Sci. U. S. A.* **1998**, *95*, 7396−7401.

(6) Castro-Camus, E.; Johnston, M. B. Conformational changes of photoactive yellow protein monitored by terahertz spectroscopy. *Chem. Phys. Lett.* **2008**, *455*, 289−292.

(7) Perman, B.; Srajer, V.; Ren, Z.; Teng, T. Y.; Pradervand, C.; Ursby, T.; Bourgeois, D.; Schotte, F.; Wulff, M.; Kort, R.; et al. Energy transduction on the nanosecond time scale: Early structural events in a xanthopsin photocycle. *Science* **1998**, *279*, 1946−1950.

(8) Rajagopal, S.; Anderson, S.; Srajer, V.; Schmidt, M.; Pahl, R.; Moffat, K. A structural pathway for signaling in the E46Q mutant of photoactive yellow protein. *Structure* **2005**, *13*, 55−63.

(9) Anderson, S.; Srajer, V.; Pahl, R.; Rajagopal, S.; Schotte, F.; Anfinrud, P.; Wulff, M.; Moffat, K. Chromophore conformation and the evolution of tertiary structural changes in photoactive yellow protein. *Structure* **2004**, *12*, 1039−1045.

(10) Kim, Y.; Ganesan, P.; Ihee, H. High-throughput instant quantification of protein expression and purity based on photoactive yellow protein turn off/on label. *Protein Sci.* **2013**, *22*, 1109−1117.

(11) Jung, Y. O.; Lee, J. H.; Kim, J.; Schmidt, M.; Moffat, K.; Srajer, V.; Ihee, H. Volume-conserving trans-cis isomerization pathways in photoactive yellow protein visualized by picosecond X-ray crystallography. *Nat. Chem.* **2013**, *5*, 212−220.

(12) Pande, K.; Hutchison, C. D. M.; Groenhof, G.; Aquila, A.; Robinson, J. S.; Tenboer, J.; Basu, S.; Boutet, S.; DePonte, D. P.; Liang, M. N.; et al. Femtosecond structural dynamics drives the trans/cis isomerization in photoactive yellow protein. *Science* **2016**, *352*, 725−729.

(13) Yang, C.; Kim, T. W.; Kim, Y.; Choi, J.; Lee, S. J.; Ihee, H. Kinetics of the E46Q mutant of photoactive yellow protein investigated by transient grating spectroscopy. *Chem. Phys. Lett.* **2017**, *683*, 262−267.

(14) Lee, K.; Kim, Y.; Jung, J.; Ihee, H.; Park, Y. Measurements of complex refractive index change of photoactive yellow protein over a wide wavelength range using hyperspectral quantitative phase imaging. *Sci. Rep.* **2018**, *8*, 3064.

(15) Baca, M.; Borgstahl, G. E. O.; Boissinot, M.; Burke, P. M.; Williams, D. R.; Slater, K. A.; Getzoff, E. D. Complete chemical-structure of photoactive yellow protein - novel thioester-linked 4-hydroxycinnamyl chromophore and photocycle chemist. *Biochemistry* **1994**, *33*, 14369−14377.

(16) Hoff, W. D.; Devreese, B.; Fokkens, R.; NugterenRoodzant, I. M.; VanBeeumen, J.; Nibbering, N.; Hellingwerf, K. J. Chemical reactivity and spectroscopy of the thiol ester-linked p-coumaric acid chromophore in the photoactive yellow protein from Ectothiorhodospira halophila. *Biochemistry* **1996**, *35*, 1274−1281.

(17) Harigai, M.; Yasuda, S.; Imamoto, Y.; Yoshihara, F.; Tokunaga, F.; Kataoka, M. Amino acids in the N-terminal region regulate the photocycle of photoactive yellow protein. *J. Biochem.* **2001**, *130*, 51−56.

(18) Harigai, M.; Imamoto, Y.; Kamikubo, H.; Yamazaki, Y.; Kataoka, M. Role of an N-terminal loop in the secondary structural change of photoactive yellow protein. *Biochemistry* **2003**, *42*, 13893−13900.

(19) van der Horst, M. A.; van Stokkum, I. H.; Crielaard, W.; Hellingwerf, K. J. The role of the N-terminal domain of photoactive yellow protein in the transient partial unfolding during signalling state formation. *FEBS Lett.* **2001**, *497*, 26−30.

(20) Putnam, C. D.; Hammel, M.; Hura, G. L.; Tainer, J. A. X-ray solution scattering (SAXS) combined with crystallography and computation: defining accurate macromolecular structures, conformations and assemblies in solution. *Q. Rev. Biophys.* **2007**, *40*, 191−285.

(21) Zagrovic, B.; Jayachandran, G.; Millett, I. S.; Doniach, S.; Pande, V. S. How large is an alpha-helix? Studies of the radii of gyration of helical peptides by small-angle X-ray scattering and molecular dynamics. *J. Mol. Biol.* **2005**, *353*, 232−241.

(22) Jacques, D. A.; Trewhella, J. Small-angle scattering for structural biology-Expanding the frontier while avoiding the pitfalls. *Protein Sci.* **2010**, *19*, 642−657.

(23) Svergun, D. I. Small-angle X-ray and neutron scattering as a tool for structural systems biology. *Biol. Chem.* **2010**, *391*, 737−743.

(24) Franke, D.; Svergun, D. I. DAMMIF, a program for rapid ab-initio shape determination in small-angle scattering. *J. Appl. Crystallogr.* **2009**, *42*, 342−346.

(25) Volkov, V. V.; Svergun, D. I. Uniqueness of ab initio shape determination in small-angle scattering. *J. Appl. Crystallogr.* **2003**, *36*, 860−864.

(26) Kozin, M. B.; Svergun, D. I. Automated matching of high- and low-resolution structural models. *J. Appl. Crystallogr.* **2001**, *34*, 33−41.

(27) Svergun, D.; Barberato, C.; Koch, M. H. J. CRYSOL - A program to evaluate x-ray solution scattering of biological macromolecules from atomic coordinates. *J. Appl. Crystallogr.* **1995**, *28*, 768−773.

(28) James, F.; Roos, M. Minuit − a system for function minimization and analysis of parameter errors and correlations. *Comput. Phys. Commun.* **1975**, *10*, 343−367.

(29) Kim, T. W.; Lee, J. H.; Choi, J.; Kim, K. H.; van Wilderen, L. J.; Guerin, L.; Kim, Y.; Jung, Y. O.; Yang, C.; Kim, J.; et al. Protein structural dynamics of photoactive yellow protein in solution revealed by pump-probe X-ray solution scattering. *J. Am. Chem. Soc.* **2012**, *134*, 3145−3153.

(30) Kim, T. W.; Yang, C.; Kim, Y.; Kim, J. G.; Kim, J.; Jung, Y. O.; Jun, S.; Lee, S. J.; Park, S.; Kosheleva, I.; et al. Combined probes of X-ray scattering and optical spectroscopy reveal how global conformational change is temporally and spatially linked to local structural perturbation in photoactive yellow protein. *Phys. Chem. Chem. Phys.* **2016**, *18*, 8911−8919.

(31) Tenboer, J.; Basu, S.; Zatsepin, N.; Pande, K.; Milathianaki, D.; Frank, M.; Hunter, M.; Boutet, S.; Williams, G. J.; Koglin, J. E.; et al. Time-resolved serial crystallography captures high-resolution intermediates of photoactive yellow protein. *Science* **2014**, *346*, 1242−1246.




DOI: 10.1021/acs.jpcb.8b01768
J. Phys. Chem. B 2018, 122, 4513−4520

(32) Ramachandran, P. L.; Lovett, J. E.; Carl, P. J.; Cammarata, M.; Lee, J. H.; Jung, Y. O.; Ihee, H.; Timmel, C. R.; van Thor, J. J. The short-lived signaling state of the photoactive yellow protein photoreceptor revealed by combined structural probes. *J. Am. Chem. Soc.* **2011**, *133*, 9395−9404.
(33) Genick, U. K.; Borgstahl, G. E. O.; Ng, K.; Ren, Z.; Pradervand, C.; Burke, P. M.; Srajer, V.; Teng, T. Y.; Schildkamp, W.; McRee, D. E.; et al. Structure of a protein photocycle intermediate by millisecond time-resolved crystallography. *Science* **1997**, *275*, 1471−1475.
(34) Harigai, M.; Kataoka, M.; Imamoto, Y. A single CH/pi weak hydrogen bond governs stability and the photocycle of the photoactive yellow protein. *J. Am. Chem. Soc.* **2006**, *128*, 10646−10647.



DOI: 10.1021/acs.jpcb.8b01768
*J. Phys. Chem. B* 2018, 122, 4513−4520